Phys. Status Solidi A **208**, No. 4, 825–828 (2011) / **DOI** 10.1002/pssa.201026659

physica status solidi a
www.pss-a.com
applications and materials science

Influence of Sb doping on optical and structural properties of ZnO by MOCVD

Jianze Zhao[1,2], Hongwei Liang*[,1], Jingchang Sun[1,3,4], Qiuju Feng[1], Shuoshi Li[1], Jiming Bian[1], Lizhong Hu[1], Guotong Du[1,4], Jingjian Ren[2], and Jianlin Liu[2]

[1] School of Physics and Optoelectronic Technology, Dalian University of Technology, Dalian 116024, P.R. China
[2] Department of Electrical Engineering, Quantum Structures Laboratory, University of California at Riverside, Riverside, California 92521, USA
[3] School of Physics and Electronic Technology, Liaoning Normal University, Dalian, Liaoning 116029, P.R. China
[4] State Key Laboratory on Integrated Optoelectronics, College of Electronic Science and Engineering, Jilin University, Changchun 130023, P.R. China

Received 21 May 2010, revised 4 October 2010, accepted 2 November 2010
Published online 11 January 2011

Keywords MOCVD, photoluminescence, Sb doping, ZnO

* Corresponding author: e-mail hwliang@dlut.edu.cn, Phone: +86 411 84707865, Fax: +86 411 84707865

Sb-doped zinc oxide (ZnO) films grown by metal organic chemical vapor deposition (MOCVD) were investigated. The influence of Sb-doping concentration on the optical and structural properties of ZnO was investigated. The deep-level emission was suppressed gradually by Sb doping. The grain size of ZnO was also increased by Sb doping. The reasons for improvement in optical and structural properties of ZnO thin films are also discussed.

1 Introduction Zinc oxide (ZnO) has been recognized as a promising material for optoelectronic devices, such as ultraviolet light-emitting diodes (LED), laser diodes (LD), and photodetectors, owing to its wide band gap of 3.37 eV and large exciton binding energy of 60 meV at room temperature [1]. Nevertheless, effective and high-quality p-type doping has been the bottleneck of practical application of ZnO. Although many groups have successfully fabricated p-type ZnO with many dopants, especially with group V elements such as N, P, As, and Sb [1–7], the doping process always leads to extra defects and degradation of optical properties, such as N doping in ZnO [8]. An effective doping technique with no degradation in ZnO quality will be advantageous for future ZnO optoelectronics application. In our previous work, p-type ZnO film was fabricated using Sb doping by metal organic chemical vapor deposition (MOCVD) [9, 10]. An interesting phenomenon was found that there was no obvious deep-level emission in photoluminescence (PL) spectra of p-type Sb-doped ZnO by MOCVD [9]. P-type doping without degradation of optical properties is very advantageous for ZnO application in optoelectronics [8]. For the future application of ZnO, it is very important to understand the mechanism of improvement in optical properties. Vanheusden et al. [11] found that Pb doping could decrease the deep-level emission as a result of grain-boundary effects in submicrometer grains of ZnO powder. In addition, Pb in ZnO could also cause strong subgap absorption to 2 eV and degradation of ZnO structural properties. Nevertheless, the growth processes of ZnO film are totally different from powder growth processes, the mechanism of Pb doping may not be the explanation for the phenomenon in Sb-doped ZnO films. In this work, the effect of Sb doping was investigated using trimethylantimony (TMSb) precursor by MOCVD. The reason for the improvement in optical and structural properties is also discussed.

2 Experimental Undoped and Sb-doped ZnO films were grown on c-plane sapphire substrates at 500 °C. Highly pure O_2, argon (Ar), and diethylzinc (DEZn) were used as oxidizer, carrier gas and zinc precursor, respectively. The mole flux of DEZn was maintained at about 1 μmol/min by controlling bubbler pressure and carrier gas flux. TMSb was chosen as the Sb-doping source. The doping concentration was changed by adjusting the flux of the carrier gas of the TMSb source. Five ZnO samples were prepared. Sample A is undoped ZnO thin film. Samples B–E are Sb-doped ZnO thin films with TMSb carrier gas flow rate of 0.05, 0.1, 0.2, and

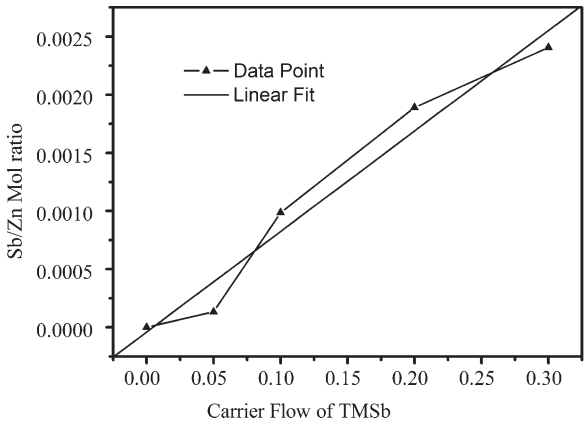

Figure 1 The EPMA curve with the Sb/Zn mol ratio versus carrier gas flow of TMSb.

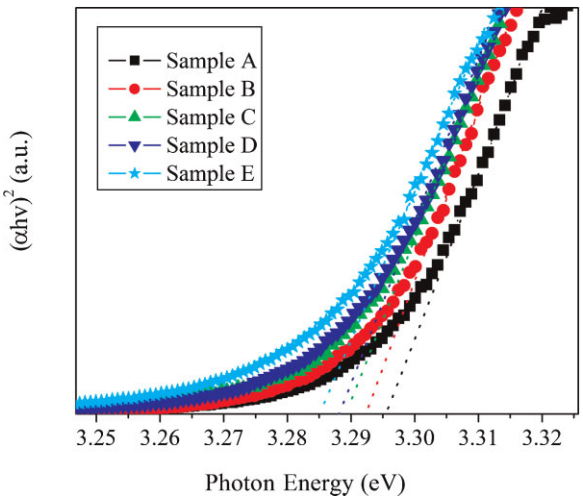

Figure 2 (online color at: www.pss-a.com) Plot of $(\alpha h\nu)^2$ versus photon energy ($h\nu$) for samples A–E.

0.3 standard-state cubic centimeter (sccm), respectively. The chemical component of samples A–E was determined by electro-probe microanalysis (EPMA). The PL measurements were performed using a He–Cd laser (325 nm) with a power of 30 mW as an excitation source and the emissions were detected by a Jobin Yvon HR320 spectrometer with a CCD detector. The optical absorption spectra were recorded using a Shimadzu UV160 spectrometer. The surface morphology was obtained by scanning electron microscopy (SEM).

3 Results and discussion Figure 1 shows the EPMA result of undoped and Sb-doped samples. The abscissa and ordinate axes represent the carrier gas flow rate of TMSb and molar ratio of Sb/Zn in ZnO films. The straight line in Fig. 1 is the linear fit curve of the data points. The Sb/Zn molar ratio in ZnO films exhibits a good linear dependence with the carrier gas flow rate of TMSb. This confirmed that Sb-doping concentration in ZnO films can be controlled linearly and accurately by adjusting the carrier gas flow rate of TMSb within a settled Sb-doping range. XRD measurements were also preformed on these samples and no phase separation was found (not shown). In addition, there was no marked difference in peak intensity and full width at half-maximum ZnO (0002) diffraction peak, although there was obvious variation in Sb-doping concentration.

The optical absorption spectra were measured and the plot of $(\alpha h\nu)^2$ versus photon energy ($h\nu$) for samples A–E are shown in Fig. 2. To determine the optical band gap, the model for direct interband transitions was used:

$$\alpha h\nu = A \times (h\nu - E_g)^{1/2}, \quad (1)$$

where A is a constant, $h\nu$ the photon energy, E_g the optical band gap, and α is the absorption coefficient [12]. In this approximation, $(\alpha h\nu)^2$ is a linear function of $h\nu$. The E_g value can be obtained by extrapolating the linear portion to the photon energy ($h\nu$) axis as illustrated in Fig. 2.

It can be seen E_g values showed a slight decrease with increasing Sb-doping concentration. The E_g value of sample A is 3.295 eV. The E_g value of sample E decreases to 3.285 eV as the Sb carrier gas flow rate increased to 0.3 sccm. Guo et al. [13] suggested that this phenomenon indicated the formation of an Sb-doping energy level in ZnO by pulsed laser deposition. Sb doping could introduce an acceptor energy level and the acceptor binding energies are at 160 and 130–140 meV, according to the theoretical calculation [14] and experimental results [1, 6], respectively [9]. Therefore, the shrinkage of E_g in the absorption spectra of Sb-doped ZnO should be partly attributed to the band-tailing effect introduced by Sb doping, which is similar to Zr-doped ZnO [15].

Figure 3 shows the PL spectra of samples A–E measured at room temperature. Because there was no obvious change in the intensity and position of near-band-edge (NBE) emission peak, the PL intensities are normalized to facilitate comparison. As shown in Fig. 3, the undoped sample (sample A) has the strongest deep-level emission around 2.1 eV. The

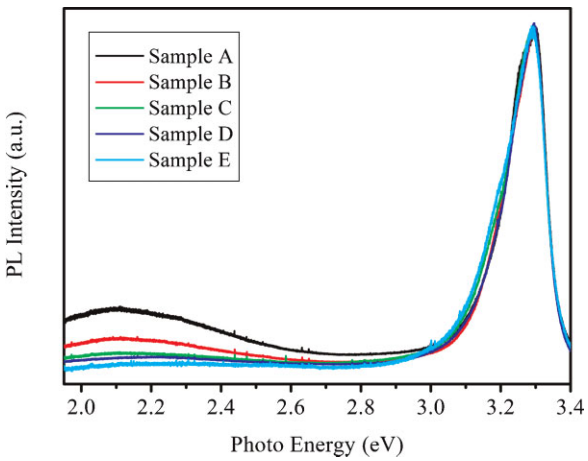

Figure 3 (online color at: www.pss-a.com) Room temperature PL spectra of samples A–E.

yellow luminescence band is usually assigned to be related to interstitial O (O_i) defects in ZnO [16, 17]. It is well known that visible emissions are generally generated by recombination related to intrinsic defects, such as O vacancies (V_O), interstitial Zn (Zn_i), Zn vacancies (V_{Zn}) and O_i [18]. V_O is related to the green luminescence around 2.4 eV, which does not coincide with any peak in Fig. 3 [19]. Zn_i is a shallow donor located at 0.22 eV below the conduction band [18, 20]. The absence of V_O and Zn_i is reasonable because there should be excess oxygen and insufficient Zn in the film at O-rich growth condition [19]. For individual V_{Zn}, it is a shallow acceptor that is usually related to emissions around 3.09 eV [21]. Furthermore, based on the theory of doping by large-size-mismatched impurities, more V_{Zn} should be introduced in Sb-doped ZnO [14]. Nevertheless, no V_{Zn}-related emissions were observed for any of the samples. So it is reasonable to conclude that the deep-level emission in Fig. 3 is attributed to O_i defects.

It can be noticed that the deep-level emissions become weaker with increasing Sb-doping concentration. Considering Sb-doping concentration is the only condition that was changed, the suppression of deep-level emissions should be attributed to Sb doping. Generally, deep-level emissions would be increased due to the defects introduced by dopants, such as Zn_i in N-doped ZnO [22, 23]. Nevertheless, Sb doping in ZnO is not simply substitution doping like N in ZnO. According to Ref. [14], the formation energy of V_{Zn} will be reduced in Sb-doped ZnO [14]. Xiu et al. [1] also observed V_{Zn} luminescence peak in PL of heavily Sb-doped ZnO by molecular beam epitaxy. Samples B–E are not heavy Sb-doped ZnO, so there is not enough V_{Zn}, which should be the reason for lack of V_{Zn} luminescence in Fig. 3. Therefore, the reason for the deep-level quenching should be the reduction of O_i defects by Sb doping.

Generally, the optical properties of ZnO films are related to the morphology of ZnO films. Therefore, the surface morphology of samples A–E was characterized by SEM to investigate the mechanism of the Sb-doping effect on optical properties. As shown in Fig. 4, the grains are dense and their dimension is relatively uniform in each sample. The grain size increases gradually with the increase of Sb-doping concentration while the morphologies become more faceted. Because the Sb-doping concentration is the only condition that was changed, the increase of grain size should be caused by Sb doping. Generally, surfactant has been used to improve the crystal quality and increase the grain size in semiconductor growth [24]. Sb has been used as a surfactant in many semiconductors [25–29], especially in GaN [24]. Zhang et al. [24] discussed the mechanism of the Sb surfactant effect on feature size, optical properties, and growth process in GaN by MOCVD. For ZnO, many elements have been suggested to be surfactants, such as Al [30] and arsenic [31]. The arsenic surfactant can reduce the total energy of the growing surface. The formation energy per O atom is 2.3 and 3.6 eV for As_2O_3 and ZnO, respectively. Like Sb in GaN, arsenic will capture O *ad atoms* to form stable AsO_2^- species that have a lower surface diffusion barrier. This can lead to a layer-by-layer growth of ZnO by MOCVD [31]. The formation energy per O atom is 2.2 eV for Sb_2O_3, which is slightly lower than it is for As_2O_3 [31]. Theoretically, this should make Sb a good surfactant for ZnO. Corinne Sartel et al. [32] also found that Sb can act as a surfactant in ZnO by MOCVD. The surfactant effect of Sb should be the reason for increasing grain size. Sb surfactant was expected to reduce the formation energy and diffusion barrier of O *ad atoms* that can increase the grain size along the substrate plane.

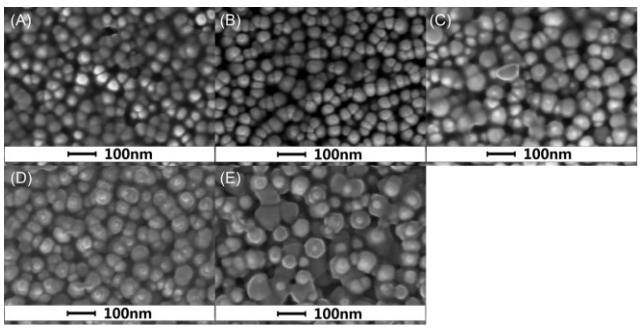

Figure 4 SEM images of samples A–E.

Similar to the cases of Sb in GaN and As in ZnO [31], Sb surfactant can affect the thermodynamic and kinetics process during ZnO MOCVD growth. Some complexes such as SbO_2^- may be comprised to indirectly increase the surface diffusion mobility of O *ad atoms* on the growth front. The mobile complexes should move quickly toward step edges, leading to Zn-rich conditions on the immediate growth front even under O-rich growth conditions. It will also greatly increase the surface diffusion length of zinc *ad atoms* [31]. The enhancement of diffusion ability of Zn and O *ad atoms* should increase the growth along the substrate direction, which leads to larger grain size, as shown in Fig. 4 [24].

Based on the mechanism above, the surfactant effect should also be one of the reasons for the enhancement of optical properties of Sb-doped ZnO. Enhancement of *ad atoms* mobility introduced by a surfactant will directly affect not only surface morphology but also the defect generation and propagation. First, the diffusion ability of Zn is improved, leading to Zn-rich conditions, which should decrease the formation of intrinsic defect O_i even under O-rich conditions. Secondly, O *ad atoms* will not tend to stay at interstice positions due to the increased mobility. Therefore, the suppression on the intrinsic defect O_i should be the reason of the quenching of yellow luminescence with the increase of Sb-doping concentration in Fig. 3. The similar Sb surfactant effect on reduction of deep levels was also observed in GaN by MOCVD [24]. The specific effect of Sb surfactant in ZnO by MOCVD still needs further investigation.

4 Conclusion In conclusion, the optical and structural properties of ZnO films were improved gradually with increase of Sb-doping concentration. The surfactant effect of Sb should be the major reason of the improvement. The Sb surfactant could improves the mobile ability of Zn and O at

the growth front, which can reduce the intrinsic defects O_i and increase the grain size. The improvement in optical and structural properties introduced by Sb is very advantageous for the future application of ZnO.

Acknowledgements This work was supported by NSFC (grant nos. 60976010, 10804040, 10804014, 60877020, 11004092, 11004020, and 61076045), Doctoral Scientific Research Starting Foundation of Liaoning province (no. 20081081). The UCR effort was supported by DOE under grant no. DE-FG02-08ER46520.

References

[1] F. X. Xiu, Z. Yang, L. J. Mandalapu, D. T. Zhao, and J. L. Liu, Appl. Phys. Lett. **87**, 252102 (2005).
[2] A. Tsukazaki, A. Ohtomo, T. Onuma, M. Ohtani, T. Makino, M. Sumiya, K. Ohtani, S. F. Chichibu, S. Fuke, Y. Segawa, H. Ohno, H. Koinuma, and M. Kawasaki, Nature Mater. **4**, 42 (2005).
[3] H. W. Liang, Y. M. Lu, D. Z. Shen, Y. C. Liu, J. F. Yan, C. X. Shan, B. H. Li, Z. Z. Zhang, J. Y. Zhang, and X. W. Fan, Phys. Status Solidi A **202**, 1060 (2005).
[4] F. X. Xiu, Z. Yang, L. J. Mandalapu, J. L. Liu, and W. P. Beyermann, Appl. Phys. Lett. **88**, 052106 (2006).
[5] Y. R. Ryu, T. S. Lee, and H. W. White, Appl. Phys. Lett. **83**, 87 (2003).
[6] E. Przezdziecka, E. Kaminska, I. Pasternak, A. Piotrowska, and J. Kossut, Phys. Rev. B **76**, 193303 (2007).
[7] X. H. Pan, Z. Z. Ye, J. S. Li, X. Q. Gu, Y. J. Zeng, H. P. He, L. P. Zhu, and Y. Che, Appl. Surf. Sci. **253**, 5067 (2007).
[8] E. Przezdziecka, E. Kaminska, K. P. Korona, E. Dynowska, W. Dobrowolski, R. Jakiela, L. Klopotowski, and J. Kossut, Semicond. Sci. Technol. **22**, 10 (2007).
[9] J. Z. Zhao, H. W. Liang, J. C. Sun, Q. J. Feng, J. M. Bian, Z. W. Zhao, H. Q. Zhang, L. Z. Hu, and G. T. Du, Electrochem. Solid-State Lett. **11**, H323 (2008).
[10] J. Z. Zhao, H. W. Liang, J. C. Sun, J. M. Bian, Q. J. Feng, L. Z. Hu, H. Q. Zhang, X. P. Liang, Y. M. Luo, and G. T. Du, J. Phys. D: Appl. Phys. **41**, 195110 (2008).
[11] K. Vanheusden, W. L. Warren, J. A. Voigt, C. H. Seager, and D. R. Tallant, Appl. Phys. Lett. **67**, 091280 (1995).
[12] J. C. Sun, J. M. Bian, H. W. Liang, J. Z. Zhao, L. Z. Hu, Z. W. Zhao, W. F. Liu, and G. T. Du, Appl. Surf. Sci. **253**, 5161 (2007).
[13] W. Guo, A. Allenic, Y. B. Chen, X. Q. Pan, Y. Che, Z. D. Hu, and B. Liu, Appl. Phys. Lett. **90**, 242108 (2007).
[14] S. Limpijumnong, S. B. Zhang, S. H. Wei, and C. H. Park, Phys. Rev. Lett. **92**, 155504 (2004).
[15] G. K. Paul, S. Bandyopadhyay, S. K. Sen, and S. Sen, Mater. Chem. Phys. **79**, 71 (2003).
[16] Y.-J. Lin, C.-L. Tsai, Y.-M. Lu, and C.-J. Liu, J. Appl. Phys. **99**, 093501 (2006).
[17] X. L. Wu, G. G. Siu, C. L. Fu, and H. C. Ong, Appl. Phys. Lett. **78**, 162285 (2001).
[18] C. H. Ahn, Y. Y. Kim, D. C. Kim, S. K. Mohanta, and H. K. Cho, J. Appl. Phys. **105**, 013502 (2009).
[19] Q. He, X. N. Wang, H. B. Wang, J. H. Zhu, H. Wang, and Y. Jiang, J. Vac. Sci. Technol. A **27**, 051231 (2009).
[20] E. G. Bylander, J. Appl. Phys. **49**, 031188 (1978).
[21] S. H. Jeong, B. S. Kim, and B. T. Lee, Appl. Phys. Lett. **82**, 162625 (2003).
[22] K. Tamura, T. Makino, A. Tsukazaki, M. Sumiya, S. Fuke, T. Furumochi, M. Lippmaa, C. H. Chia, Y. Segawa, H. Koinuma, and M. Kawasaki, Solid State Commun. **127**, 265 (2003).
[23] Q. R. Ou, K. Shinji, A. Ogino, and M. Nagatsu, J. Phys. D: Appl. Phys. **41**, 20 (2008).
[24] L. Zhang, H. F. Tang, J. Schieke, M. Mavrikakis, and T. F. Kuech, J. Appl. Phys. **92**, 052304 (2002).
[25] A. Portavoce, I. Berbezier, and A. Ronda, Phys. Rev. B **69**, 155416 (2004).
[26] C. S. Peng, Q. Huang, W. Q. Cheng, J. M. Zhou, Y. H. Zhang, T. T. Sheng, and C. H. Tung, Appl. Phys. Lett. **72**, 202541 (1998).
[27] J. K. Shurtleff, R. T. Lee, C. M. Fetzer, and G. B. Stringfellow, Appl. Phys. Lett. **75**, 131914 (1999).
[28] J. K. Shurtleff, S. W. Jun, and G. B. Stringfellow, Appl. Phys. Lett. **78**, 203038 (2001).
[29] T. Kageyama, T. Miyamoto, M. Ohta, T. Matsuura, Y. Matsui, T. Furuhata, and F. Koyama, J. Appl. Phys. **96**, 44 (2004).
[30] R. Cebulla, R. Wendt, and K. Ellmer, J. Appl. Phys. **83**, 021087 (1998).
[31] J. D. Ye, S. T. Tan, S. Pannirselvam, S. F. Choy, X. W. Sun, G. Q. Lo, and K. L. Teo, Appl. Phys. Lett. **95**, 101905 (2009).
[32] N. H. Corinne Sartel, A. Lusson, J. M. Laroche, P. Galtier, and V. Sallet, E-MRS Fall Meeting, 2009.

